Spring 5-7-2022

Th1, Th2, and TH17 Inflammatory Pathways Predict Cardiometabolic Protein Expression in Serum of Covid-19 Patients

James Richard Michels

TH1, TH2, AND TH17 INFLAMMATORY PATHWAYS PREDICT CARDIOMETABOLIC PROTEIN EXPRESSION IN SERUM OF COVID-19 PATIENTS

By

James Richard Michels

A thesis submitted to the faculty of The University of Mississippi in partial fulfillment of the requirements of the Sally McDonnell Barksdale Honors College.

Oxford, MS

May 2022

Approved By

Advisor: Dr. Ana Pavel

Reader: Dr. Glenn Walker

Reader: Dr. Nikki Reinemann

ACKNOWLEDGEMENTS

I would like to thank Dr. Ana Pavel for introducing me to computational immunology and bioinformatics, starting me on a path leading to where this thesis is today. I would additionally like to thank Mohammad Shaheed Nazrul, Sudeep Adhikari, and Dawn Wilkins for their vital contributions towards the research described in this thesis, as well as Glenn Walker and Nikki Reinemann for their help as readers for this capstone project.

ABSTRACT

JAMES RICARD MICHELS: Th1, Th2 and Th 17 inflammatory pathways predict cardiometabolic protein expression in serum of COVID-19 patients.

(Under the direction of Ana Pavel)

A predominant source of complications in SARS-CoV-2 patients arises from severe systemic inflammation contributed to by Helper T-cell associated cytokines, potentially leading to tissue damage and organ failure. The high inflammatory burden of this viral infection often results in cardiovascular comorbidities. A better understanding of the interaction between the cytokine storm and cardiovascular proteins might inform medical decisions and therapeutic approaches. We hypothesized that all major helper T-cell inflammatory pathways (Helper T 1, Helper T 2 and Helper T 17) synergistically contribute to cardiometabolic pathways in serum of COVID-19 patients, and that both of these factors correlate to COVID-19 severity. We found that Helper T 1, Helper T 2, and Helper T 17 cytokines and chemokines are able to predict expression of 186 cardiometabolic proteins profiled by OLINK proteomics.

TABLE OF CONTENTS

LIST OF FIGURES

LIST OF ABBREVIATIONS

COVID-19	Coronavirus disease 2019
FCH	Fold Change Value
logFCH	Logarithmic Fold Change Value
p	p-value
SARS-CoV-2	Severe Acute Respiratory Syndrome Coronavirus 2
Th1	Helper T 1 cells
Th17	Helper T 17 cells
Th2	Helper T 2 cells

CHAPTER 1

INTRODUCTION

COVID-19 disease, since its discovery in 2019, has caused a large amount of damage throughout the world, resulting in massive strain on hospital systems, and, sadly, many patient deaths (Satiani et al., 2020). A major point of study is through patient proteomic profiles, which consists of chemical signals such as cytokines and chemokines (Stenken et al., 2016). Patient proteomic profiles, in conjunction with computational analysis through correlation methods can be used to gain a greater understanding of the interactions of these chemical signals in inflammatory diseases. This could allow for the enhanced development of therapies to prevent the cardiovascular complications such as myocardial strain and hypertension associated with associated proteins or the cytokines (Del Valle et al., 2020).

This study explores how the presence of cardiometabolic proteins and helper T cell associated cytokines and chemokines from day zero data affect patient outcomes. The dataset that is being used in this analysis originates from the Massachusetts General Hospital COVID-19 Registry, and the study takes a large number of patient proteomic profiles being analyzed through computational modelling in order to correlate the presence of markers and proteins with patient severities versus a control group (Pavel et al., 2021). After this, the cytokines and chemokines are modelled in relation to cardiometabolic proteins in order to create a set of networks that will map the large number of signals that take part in the activation or suppression of these cardiometabolic proteins.

CHAPTER 2

BACKGROUND

2.1 COVID-19

2.1.1 COVID-19 BACKGROUND

The respiratory virus SARS-CoV-2 has caused over 200 million reported cases of COVID-19 Disease and over 5 million reported deceased to date (Dong et al., 2020). Strides have been made in the treatment of this virus through the development of the vaccinations to prevent infection and specialized treatments such as the monoclonal antibody infusions (Brobst et al., 2022). Despite this, more research into the treatment of COVID-19 is needed, as there are many dangerous complications such as acute respiratory distress syndrome, respiratory failure, hepatic and renal insufficiency in severe cases (Yang et al., 2021). Cardiovascular complications such as hypertension and myocardial injury have also been shown in severe COVID-19 cases, and are the main interest of this study (Guo Tao et al., 2020). Proteomic profiling is a method that can study the cytokines and chemokines in the cardiometabolic system to potentially open doors for the development of immunomodulatory therapies in the future (Yu et al., 2021).

2.1.2 ROLE OF CYTOKINES AND CHEMOKINES IN COVID-19

Cytokines and chemokines, often referred together as markers, are signal molecules released by Helper T cells in an immune response (Dong, C et al., 2021). Each type of Helper T immune cell reacts to a different potential threat to the body. The three Helper T cells that are the focus of this study are selected for their implications in the body's reaction to COVID-19. Helper

T 1 cells react to viruses (Alberts et al., 2002), Helper T 2 cells react to antigens such as the COVID-19 spike protein (Wu et al., 2021), and Helper T 17 cells play a role in adaptive immunity (Khader et al., 2009), often acting in coordination with the Helper T cells during an autoimmune response.

Recent research has shown that a shift in the balance of Helper T 1 and Helper T 2 associated markers, with an increase in Helper T 2 expression, is correlated with an increase in severity in COVID-19 (Pavel et al., 2021). Research on atopic patients also has shown that patients treated with Helper T 2 inhibitors have displayed more asymptomatic cases (Ungar et al., 2022).

The study of cytokines and chemokines is fundamental towards understanding the body's reaction to viral infection by COVID-19 because these signals play a key role in the reaction and possible overreaction in the immune system. In this process referred to as cytokine storm, there is an elevated expression of inflammatory helper-T-cell-associated cytokines (Fajgenbaum et al., 2020). Many effects of the COVID-19 disease are believed to be as a result of cytokine storm, and this can lead to complications. Expressed proteins that have been associated with negative side-effects are expressed more, and this can worsen a patient's condition. In the DISCUSSION section, more is discussed on proteins' effects on patients. However, cytokine storm is not necessary for complications to occur. Figure 2.1 shows an infographic on cytokine storm.

Cytokines and chemokines are deeply involved in the body's processes involved in the reaction to COVID-19 through response pathways. Response pathways describe the roles cytokines play in the complex interactions of viral infection. These pathways can be incredibly detailed, with databases such as the regularly updated KEGG PATHWAY Database (Kanehisa et al., 2000) displaying the many cytokines and chemokines involved in the process of COVID-19 infection, such as the example in Figure 2.2.

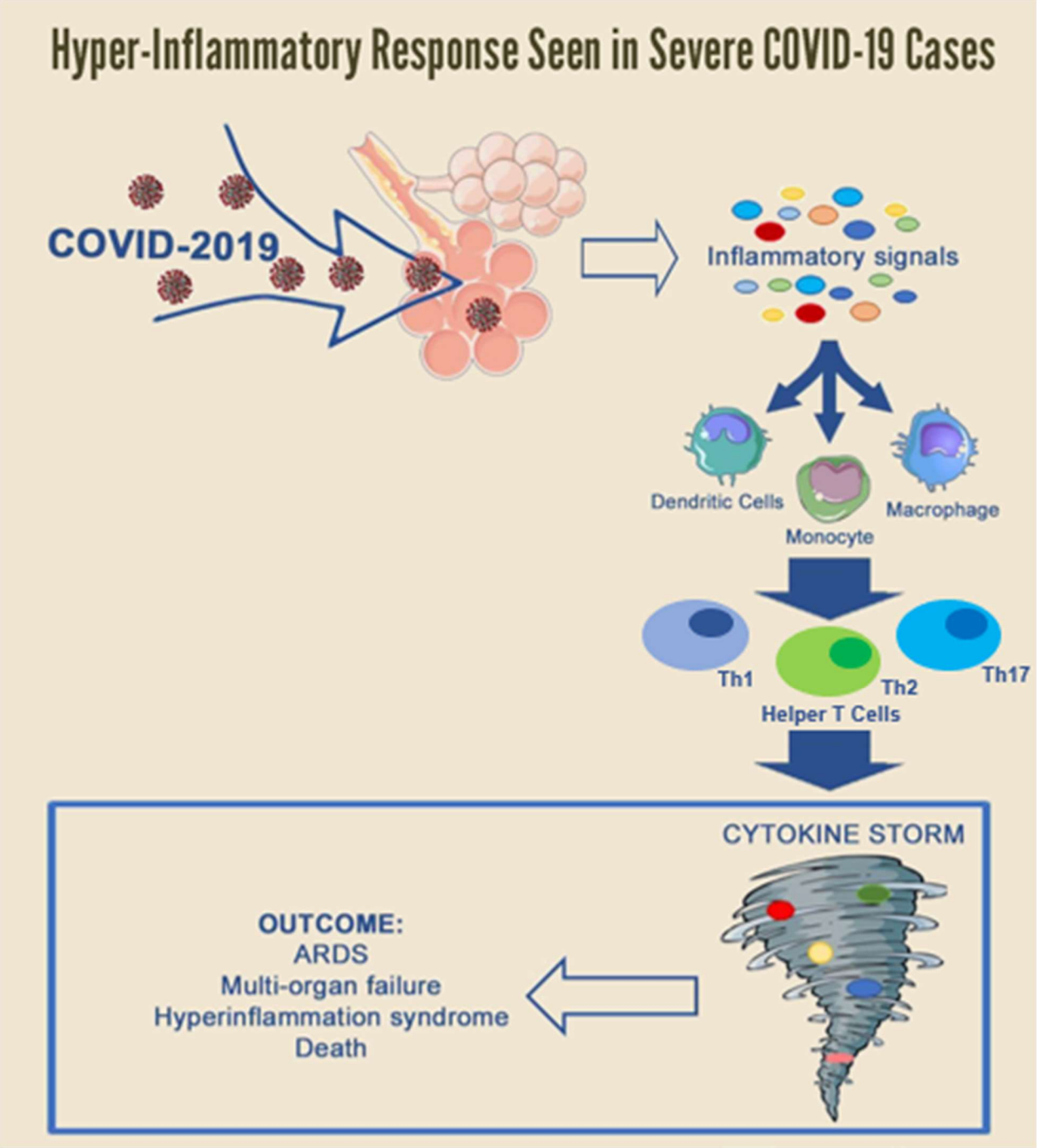

Figure 2.1: Cytokine Storm Infographic (Modified from Al-Kuraishy et al. 2020)

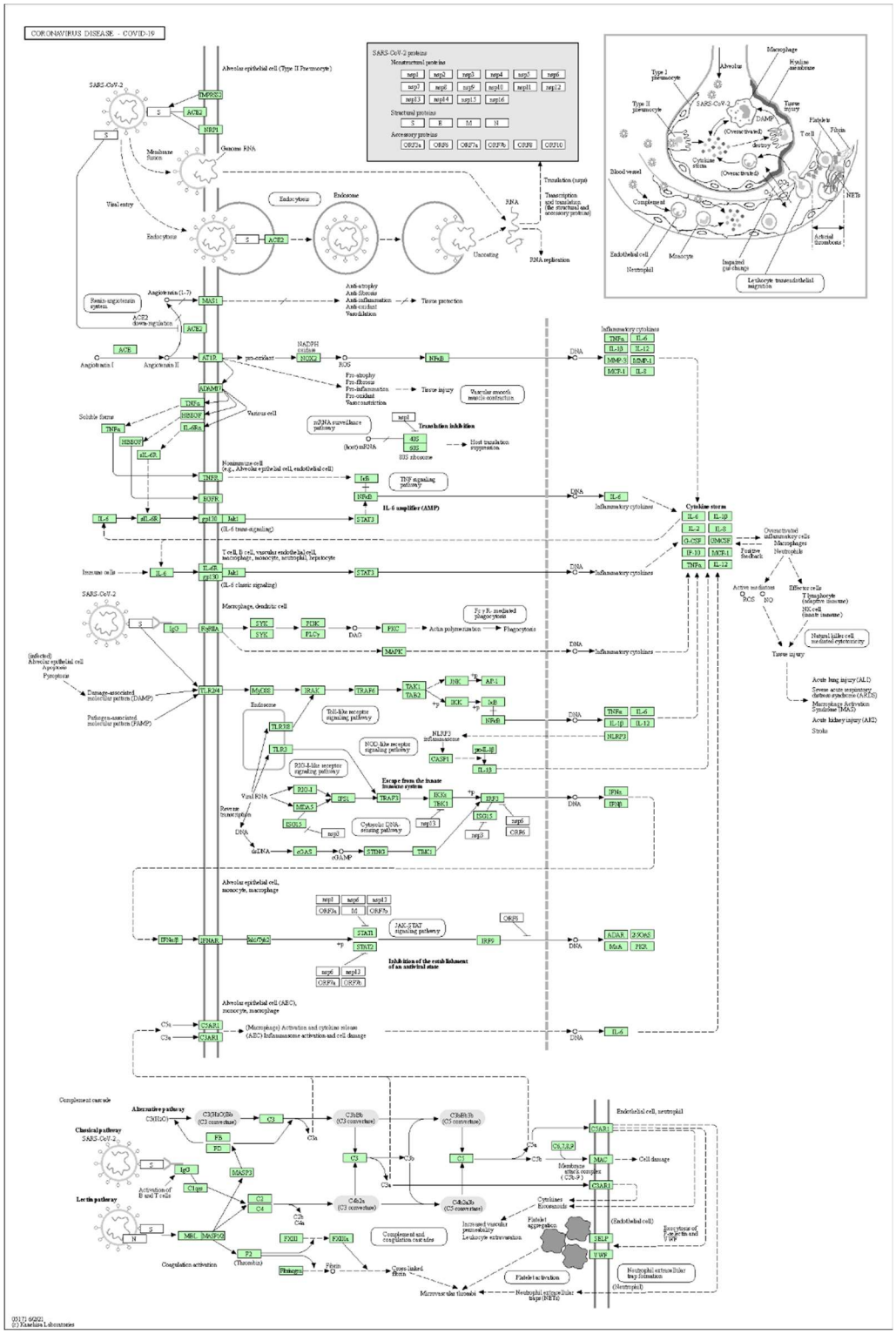

Figure 2.2 COVID Pathway from KEGG Database (Kanehisa et al., 2000)

2.2 PROFILING METHOD

The cytokines and proteins to be studied were profiled by the OLINK Explore 1536 Proteomics Assay. The OLINK Explore 1536 Proteomics Assay originally released in the summer of 2020, and is used for the screening of protein biomarkers (Olink 2021). The assay measures over 1500 proteins in 88 samples with less than 3 microliters of sample each (Olink 2021). The platform uses a semi-automated process where robots perform the entire assay except for plate transfer and sealing (Olink 2021). The automation makes the experiment repeatable and reproducible. The four panels of focus are inflammation, oncology, neurology, and cardiometabolic proteins (Olink 2021). Of these four panels, cardiometabolic proteins are of interest in the study, as no prior study has used integrated major Helper T pathways to evaluate the implications of COVID-19 cytokine expression on cardiometabolic proteins.

CHAPTER 3

DATASET

3.1 DATASET ORIGIN

The dataset originates from a Massachusetts General Hospital system study, with the data on 383 patients being collected on September 2020. The first study analyzed this dataset in order to generate a model of immune and epithelial cell interactions that are involved in cell-specific or tissue-specific damage in cases of COVID-19 (Filbin et al., 2020). The research described in this thesis is intended to analyze the cardiometabolic interactions that shape the body's response to COVID-19.

3.2 PARAMETERS

The data was obtained in two datasets, a clinical info dataset and a blood marker dataset. The recorded parameters in the clinical info dataset included the following:

- Subject ID of the Patient
- COVID status of the Patient
- Age Group of the Patient
- BMI Group of the Patient
- Presence of other conditions such as diabetes or kidney disease
- Presence of certain symptoms
- Disease severity

The severity was checked at 0, 3, 7, and 28 days after admission into the hospital system.

The blood marker dataset contained the results of the OLINK Explore 1536 Proteomics assays, which contained the limit of detection, the threshold for a valid reading from the assay, and normalized protein expression, the expressed level of a tested protein, for the presence of cardiometabolic proteins and Helper T-associated markers. The main focus of the research project described in this thesis was on the day zero data, COVID-19 status, and normalized protein expression readings.

3.3 PRELIMINARY CHANGES TO THE DATASET

The data was modified in a myriad of ways to make the managing of the data less complicated. One modification was the removal of one patient, patient number 365, for missing a normalized protein expression value for the Interferon Gamma 1 marker, IFNGR1. Every other patient displayed readable normalized protein expression levels for every other cardiometabolic protein of interest.

Another modification was changing the outcome severity scale from a five-point scale, as displayed in Figure 3.1, to a three-point scale. The intent of this change was to simplify the five-point scale, with level 3 (hospitalized with supplemental oxygen), 4 (hospitalized without supplemental oxygen), and 5 (discharged from emergency department), being merged into one "non-severe" outcome group as these levels, albeit admitted to the hospital, were not severe enough to warrant intubation. This was to simplify the patient groups so that the heatmaps could be simplified and that three groups could be focused on in the research: Deceased, Intubated, and Non-severe.

In the code that processed the data, the data was also processed at points to separate the COVID-19 Positive and COVID-19 Negative patients, so that the proteomic data of the individual groups could be processed. This would allow the COVID-19 Negative patients to act as a control group, with the COVID-19 Positive patients to act as the experimental group.

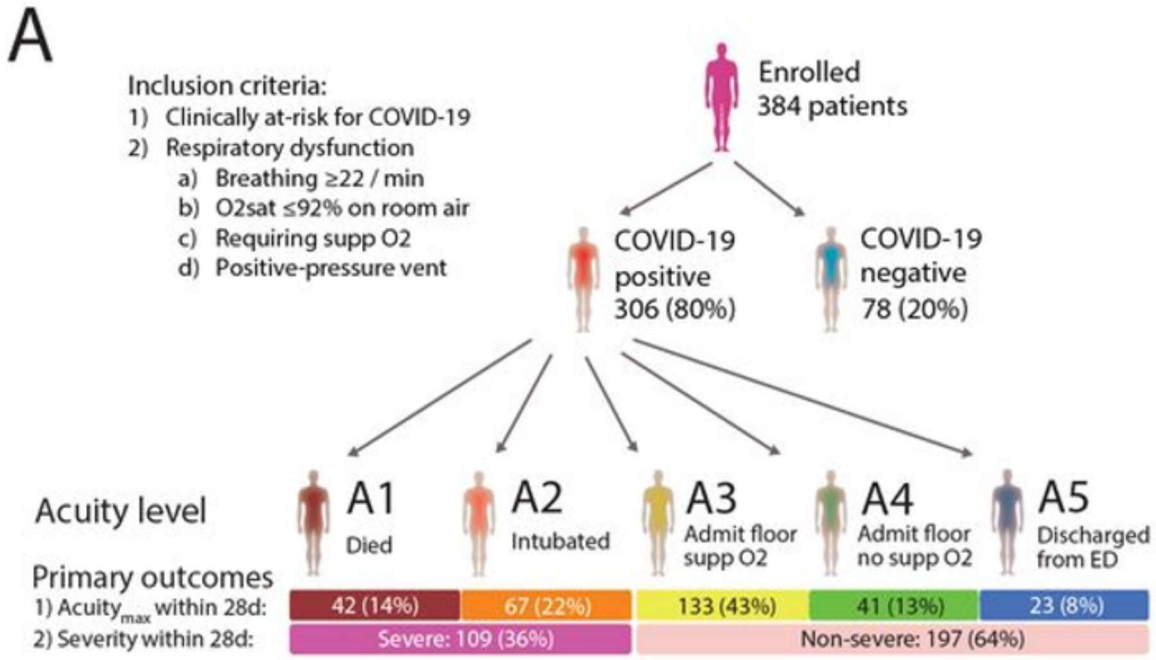

Figure 3.1: Original Five Point Scale from the Massachusetts General Hospital Study

(Filbin et al. 2020)

3.4 STATISTICS ON EXPERIMENTAL AND CONTROL GROUPS

The patients were separated into COVID-19 Positive and COVID-19 Negative groups, with 306 and 78 patients respectively. The original study from which the dataset originated found that the COVID-19 Positive patients displayed a younger median age as compared to the COVID-19 Negative patients, with median ages for each group of 58 and 67 years, respectively (Filbin et al., 2020). The COVID-19 Positive patients in this study were also found to be mostly Hispanic,

with 54% of the COVID-19 Positive group being Hispanic as compared to 15% of the COVID-19 Negative group (Filbin et al., 2020).

The patients of the study, as classified by severity, were grouped into 49 deceased patients, 83 intubated patients, and 251 non-severe patients. Of the 49 deceased patients, 42 were COVID-19 Positive and 7 were COVID-19 Negative. Of the 83 intubated patients, 67 were COVID-19 Positive and 16 were COVID-19 Negative. Of the 251 non-severe patients, 196 were COVID-19 Positive, and 55 were COVID-19 Negative.

CHAPTER 4

METHODOLOGY

4.1 CYTOKINE/CHEMOKINE SELECTION AND VARIABLES

The Helper T 1, Helper T 2, and Helper T 17 cytokines and chemokines were classified based on previous study in various inflammatory diseases for their characterized pathways and response to different targeted biologics (Pavel et al., 2021). The following cytokines and chemokines were detectable by the OLINK Explore Proteomics Assay:

- 11 Helper T 1 markers: CCL3, CCL6, CXCL11, CXCL10, CXCL9, IL2RA, IFNG, IFNGR1, IFNGR2, IL12B, and IL1B
- 14 Helper T 2 markers: CCL11, CCL13, CCL17, CCL22, CCL24, CCL26, CCL7, IL10, IL13, IL33, IL4R, IL5, IL7R, and TSLP
- 13 Helper T 17 markers: CCL20, S100P, IL6, IL6R, LCN2, S100A12, CXCL1, PI3, IL17A, IL17F, CXCL3, IL12A, and IL12B

These cytokines and chemokines were used in the study as the markers to be correlated with cardiometabolic proteins expression and patient outcomes for both the COVID-19 Positive and COVID-19 Negative groups. There are three main correlations of focus studied in this research, each with their own independent and dependent variables: The correlation between cardiometabolic protein expression (dependent variable) and cytokines/chemokine expression (independent variables), the correlation between cytokine/chemokine expression (dependent

variable) and disease severity (independent variable), and the correlation between cardiometabolic protein expression (dependent variable) and disease severity (independent variable).

4.2 R PACKAGES USED

All statistical analyses for this study were performed using the R programming language. A functionality of R that was instrumental to the data processing was the use of external R packages. Packages are extensions of R that contain specific functions and data sets suited towards different needs, and can be downloaded from within the R program. After packages are downloaded onto the RStudio client, they can be called from a directory called "library", which allows them be called for use. Further discussed below are the R packages used, and the role which each package played within the generation of the results.

4.2.1 GLMNET – LINEAR MODELLING

The glmnet R package is a package designed for lasso and other generalized linear models to perform linear regression (r-project 2021). The glmnet R package was used to perform the generalized linear models that were required for the correlations. The package's cv.glmnet function was used to predict the expression levels of each cardiometabolic protein based on Helper T 1, Helper T 2, and Helper T 17 cell immune profiles using 10-fold cross-validation. The model can be summarized by using the following equation:

$$y_{cardio} = \sum_{i=1}^{11} a_i * th1_i + \sum_{i=1}^{14} b_i * th2_i + \sum_{i=1}^{13} c_i * th17_i$$

y_{cardio} is a continuous variable representing the predicted expression of each cardiometabolic protein modelled by a weighted sum across the Helper T 1, Helper T 2, and Helper

T 17 cytokines and chemokines. The weights of the model, represented by a_i, b_i, and c_i, are estimated by the elastic net regularized linear regression. The best fit of linear predictions was calculated by Pearson correlation between the predicted and measured expression of each cardiometabolic protein. These predictions were then ranked among all 355 cardiometabolic proteins and were considered as a significant best fit if those predictions had an r value greater than or equal to 0.7, and an adjusted p-value less than 0.05.

4.2.2 IGRAPH – NETWORK GENERATION

The igraph R package contains network analysis tools that are used in order to efficiently generate network graphs, which allow connections or correlations in data to be visually displayed (igraph 2020). The igraph R package was used to visualize the interaction between immune and cardiometabolic markers with a Pearson correlation r value greater than or equal to 0.7. The edges of the networks generated represent non-zero coefficients of the elastic net regression model with an absolute value greater than or equal to 0.05. This choice was to filter noise and very weak interactions. These generated networks were additionally color-coded by changing the color of certain vertices.

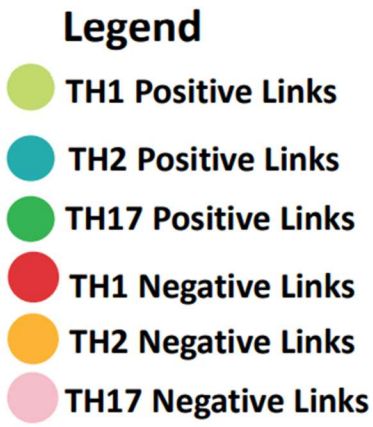

Figure 4.1: Planned Network Cytokine and Chemokine Legend

The color scheme, as displayed in Figure 4.1, allows for both positive and negative links between cytokine or chemokine and cardiometabolic protein to be identifiable, as well as clearly differentiating which Helper T cell the cytokine or chemokine is associated with.

4.2.3 GGPLOT2 – BAR GRAPH GENERATION

The ggplot2 R package is used for creating graphics, with a high degree of customizability available to the user (tidyverse). It was used in this study to generate supplementary Pearson scatterplots and in addition to a bar graph displaying the number of both positive and negative links associated with the three studied types of Helper T cells and cardiometabolic proteins.

4.2.4 DPLYR – GRAMMAR AND CONSISTENCY

The dplyr R package is used for data manipulation, and adds a consistent set of verbs to allow users to manipulate data in R more effectively. This was mainly a quality-of-life package used in the study, but was still important in isolating certain parameters of the markers, such as the subject ID, assay type, and normalized protein expression.

4.3 LASSO REGRESSION

Lasso regression, or Least Absolute Shrinkage and Selection Operator regression, is a type of linear regression that is characterized by the use of shrinkage, where data values are shrunk towards a central point, often a mean (Great Learning 2021). This method encourages models that are less complex and have fewer parameters (Great Learning 2021). Lasso regression was used in the generation of the correlations between cytokine expression and cardiometabolic protein expression modelled in the heatmaps and networks.

4.4 SUPPLEMENTAL DATA GENERATION

Supplemental data tables were generated to contain the raw values of the results of the main analysis, in the form of the mean expression of each cytokine/chemokine and cardiometabolic protein for each of the three patient groups and the logFCH, FCH, and p-values for all comparisons between the groups. This was performed for both the COVID-19 Positive group and the COVID-19 Negative group, as to show the data that is mainly implicated in the generation of heatmaps and network plots.

The logFCH and FCH values are numerical means of measuring how much a quantity changes between two measurements, which are the two compared patient groups (RDocumentation 2021). The FCH value is alternatively recorded in a logarithmic format with a base of two. The p-value is a statistic that refers to the likelihood of the data occurring under a null hypothesis, which is a hypothesis stating that there is no difference between the tested groups (Tanha et al., 2017). A significantly small p-value, a p-value less than 0.05, is considered ideal in confirming the differences between any of the major three comparisons: Deceased versus Non-severe, Intubated versus Non-severe, and Deceased versus Intubated.

CHAPTER 5

RESULTS

5.1 HEATMAPS

5.1.1 CYTOKINE AND CHEMOKINE HEATMAPS

The cytokines and chemokines of the studied Helper T cell types were analyzed via heatmaps in both COVID-19 Positive and COVID-19 Negative patients, shown in Figures 5.2 and 5.1, respectively. The heatmaps feature a color scale to display results, where a deeper red color correlates to increased cytokine or chemokine expression, and a deeper blue color correlates to a decreased cytokine or chemokine expression. The score is normalized to a z-scale, which is a color scale from -1.5 to 1.5 standard deviations from the mean, with a negative standard deviation meaning a standard deviation towards under-expression. This z-scale is displayed in Figure 5.3.

In most of the Helper T 1 and Helper T 17 markers, an increasing trend in protein expression and COVID-19 severity was shown. This increasing trend has been displayed in over half of the Helper T 2 markers as well. Significant increases, as denoted by a p-value < 0.05, were found in a myriad of markers in deceased patients as compared to non-severe patients. These significant markers are IFNGR1, CCL3, CCL4, CCL5, CXCL9, CXCL10, IL1B, and IL2RA for Helper T 1 markers, CCL11, CCL13, CCL7, CCL24, and IL4R for Helper T 2 markers, and S100A12, S100P, CCL20, LCN2, PI3, CXCL1, IL17A, and IL6 for Helper T 17 markers. COVID-

19 Negative patients did not display any significant increasing trends in deceased patients as compared to non-severe patients in the Helper T 1, Helper T 2, and Helper T 17 pathways.

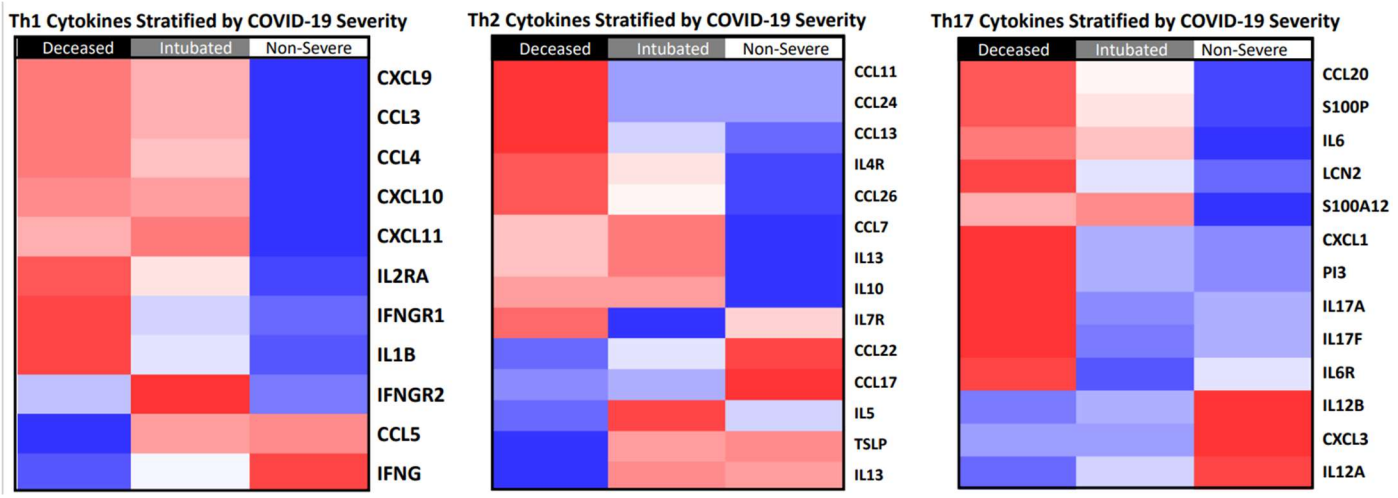

Figure 5.1: COVID-19 Group Marker Heatmaps

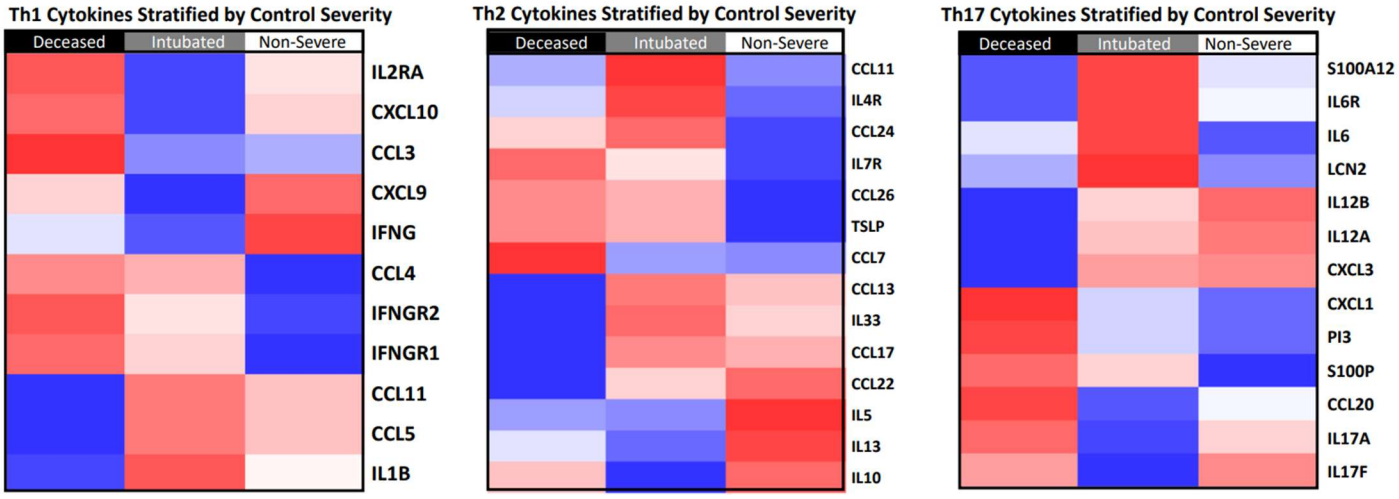

Figure 5.2: Control Group Marker Heatmaps

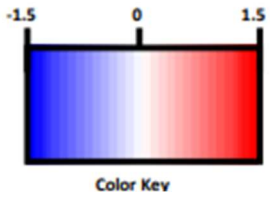

Figure 5.3: Heatmap Color Key

5.1.2 CARDIOMETABOLIC PROTEIN HEATMAP

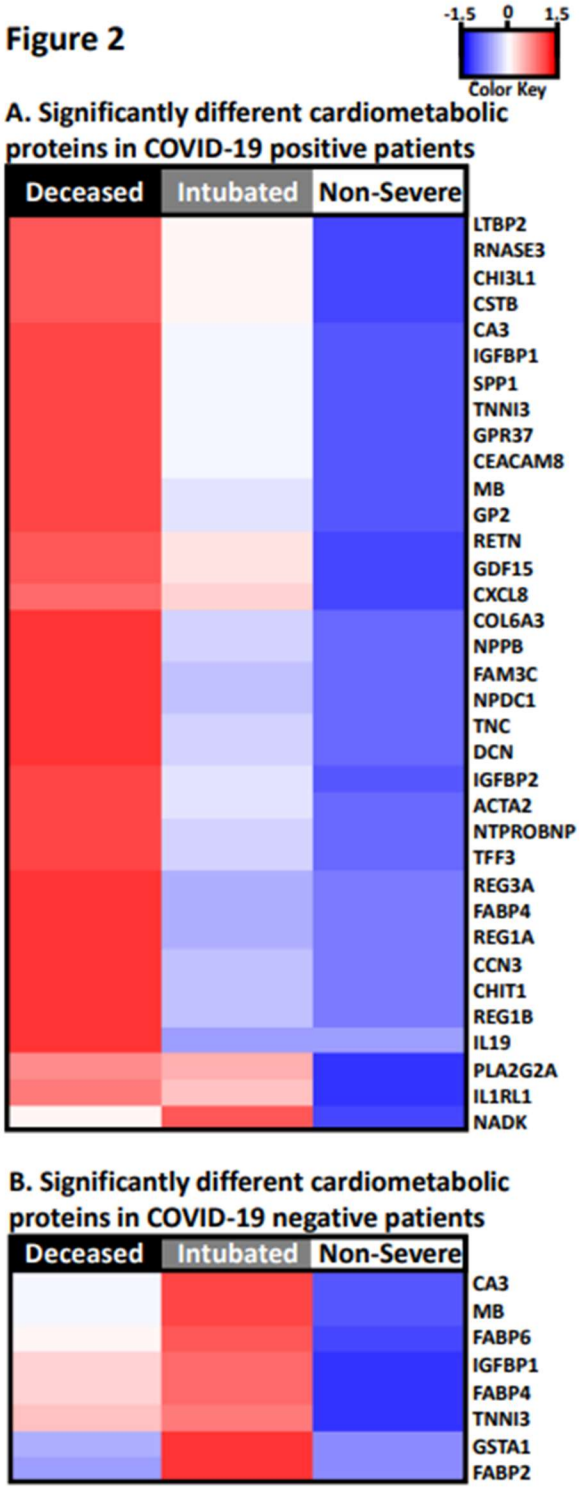

Figure 5.4: Significant Cardiometabolic Protein Heatmaps

Of the 355 cardiometabolic proteins detected by the OLINK Explore Proteomics assay, 35 cardiometabolic proteins were significantly associated with COVID-19 severity in COVID-19 Positive patients, as judged by a fold change value greater than or equal to 2, and an FDF value less than 0.05 in any of the three comparisons: deceased versus non-severe, intubated versus non-severe, or deceased versus intubated.

A heatmap, shown in Figure 5.4, was generated to display the estimated mean expression of the significant 35 cardiometabolic proteins stratified by COVID-19 severity. Notably, all 35 of the significantly expressed proteins were significantly increased in deceased versus non-severe COVID-19 Positive patient groups. Of the cardiometabolic proteins, LTBP2, RNASE3, CHI3L1, CSTB, RETN, GDF15, CXCL8, PLA2G2A, IL1RL1, and NADK all showed significantly elevated expression in intubated COVID-19 Positive patient groups versus non-severe patient groups.

Additionally, a heatmap was generated for the 8 cardiometabolic proteins that were significantly associated with severity in the COVID-19 Negative group, as defined by the same criteria as the COVID-19 Positive significant cardiometabolic proteins. Notably, none of the 8 proteins have yielded significance when comparing the deceased versus non-severe patient groups, and all of the 8 significant cardiometabolic proteins only displayed significance when comparing the intubated versus non-severe COVID-19 Negative patient groups.

5.2 NETWORKS

Network graphs were generated of the 186 expressed cardiometabolic proteins to display the interactions between the Helper T cytokines/chemokines and the cardiometabolic proteins. Figure 5.5 displays examples of some of these network graphs. The network graphs appear as

many small colored vertices, representing the Helper T cytokines and chemokines, connected to a large white vertex, representing a cardiometabolic protein. The vertices are all labelled as to identify the markers protein, and the colors on the cytokines or chemokines correlate to which Helper T cell that is associated with the cytokine or chemokine.

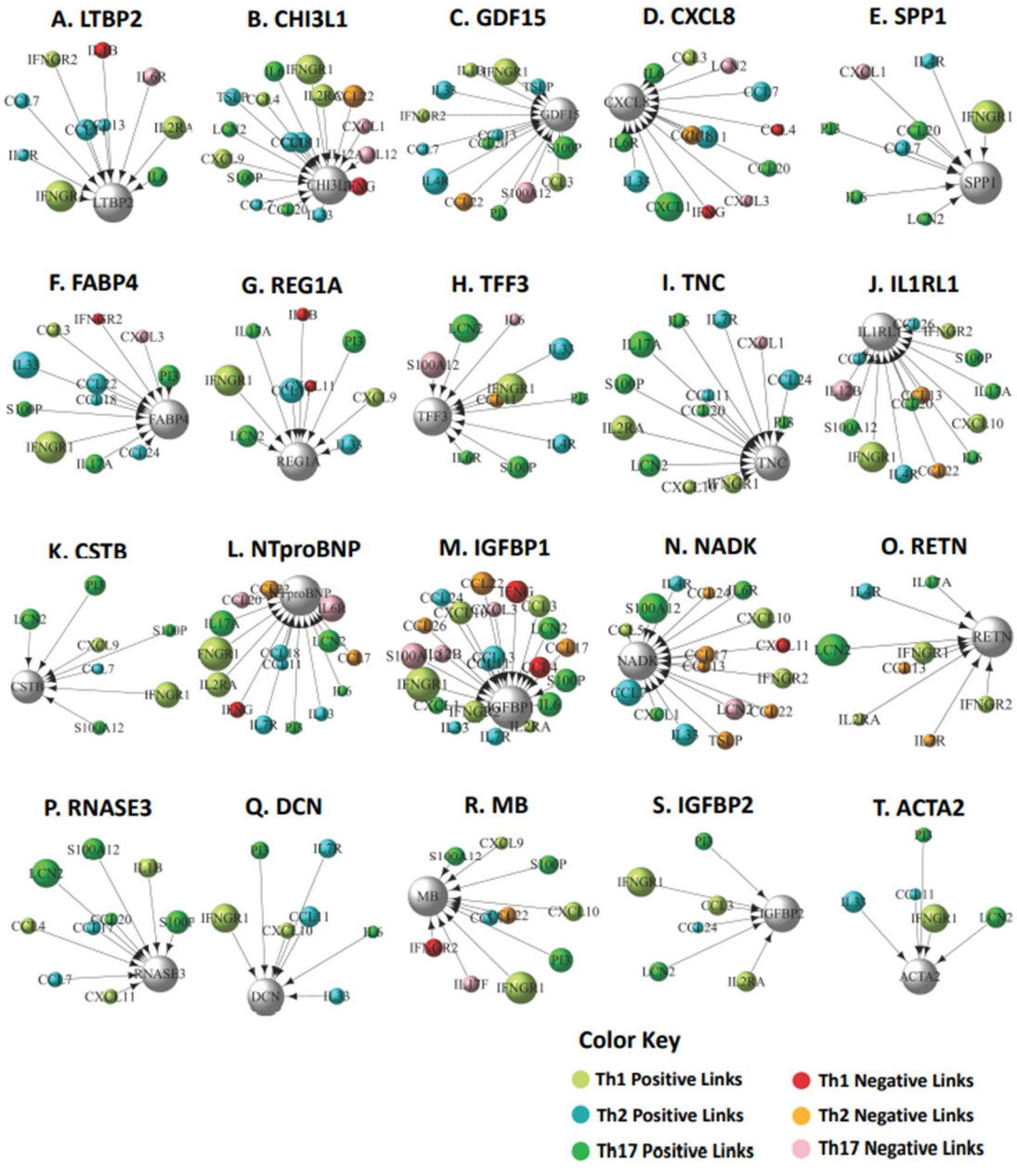

Figure 5.5: Example Significant Networks

Interestingly, a majority of links involved in these network plots are positive connections, which means that the presence or expression of that cytokine or chemokine encourages the expression of the cardiometabolic protein. This suggests that increased production in cytokines and chemokines may stimulate the overall production of cardiometabolic proteins in response to COVID-19 infection, which may correlate to increased side-effects associated with these proteins.

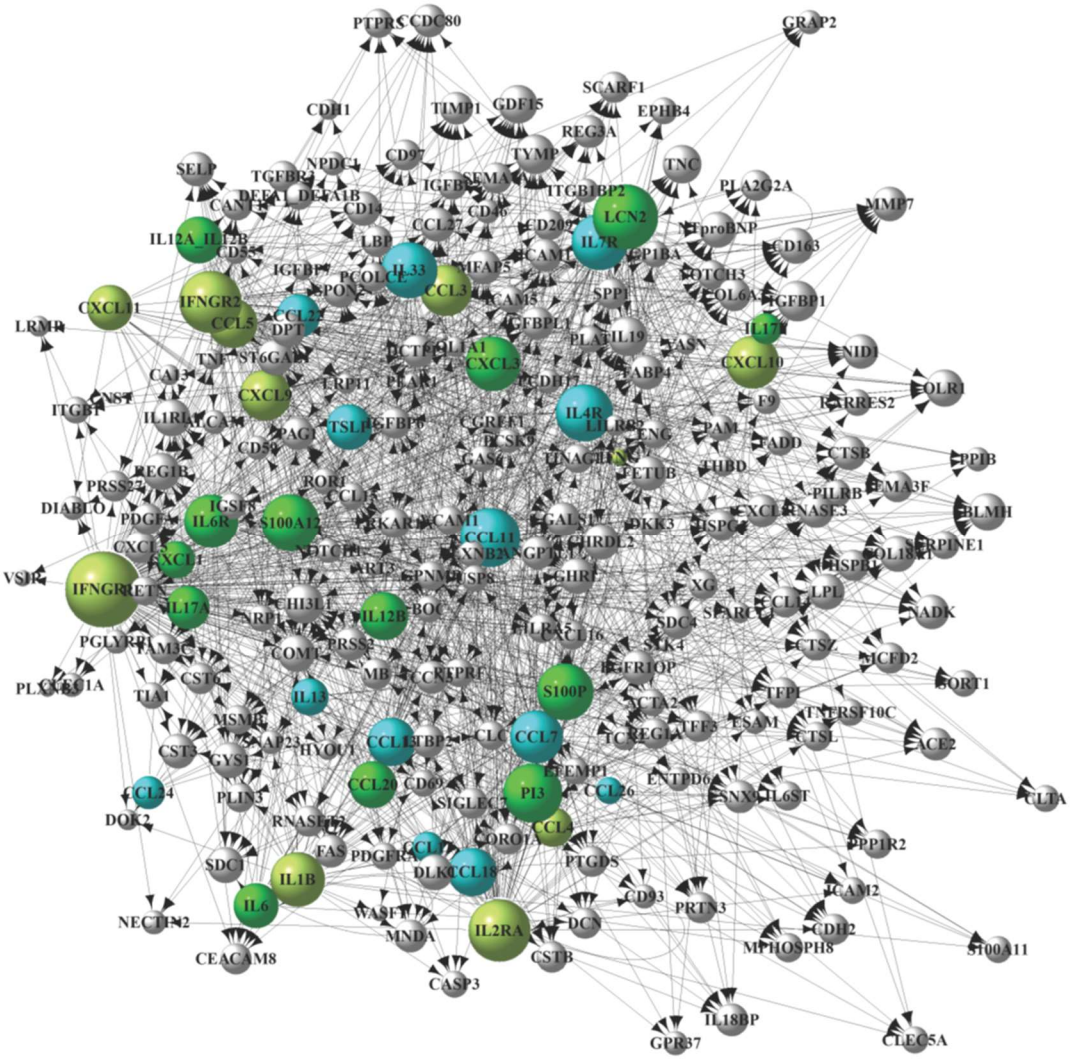

Figure 5.6: Overall Cardiometabolic Activation Network.

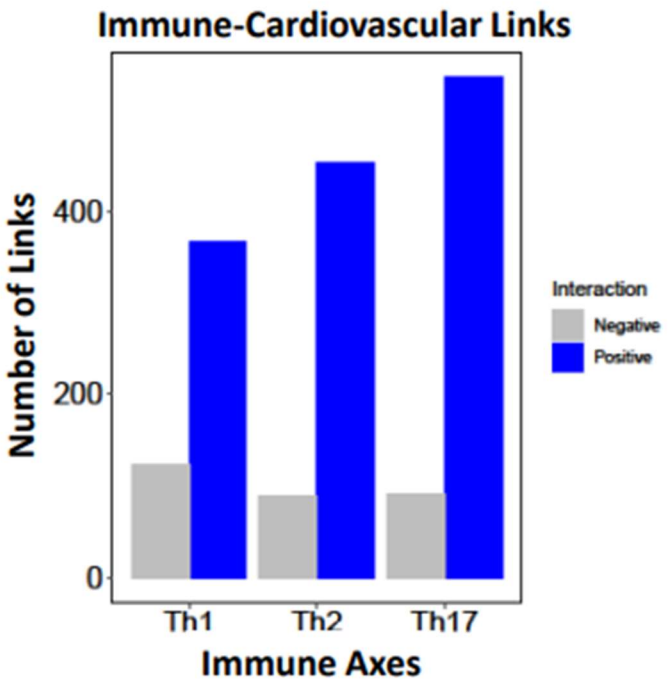

Figure 5.7: Overall Cardiometabolic Network Bar Graph

Another network graph, shown in Figure 5.6, generated was to display all positive associations in a way to display the positive connections between cytokines or chemokines and cardiometabolic proteins. The size of the colored vertices, which represent cytokines or chemokines, correlate to the number of cardiometabolic proteins that the cytokine or chemokine is positively linked to. A bar graph, shown in Figure 5.7, was created to enumerate the number of positive, or activating, and negative, or suppressing, links between the cytokines or chemokines and cardiometabolic proteins of interest. 367 positive links and 122 negative links are associated with Helper T 1 cytokines or chemokines. 452 positive links and 90 negative links are associated with Helper T 2 cytokines or chemokines. 546 positive links and 91 negative links are associated with Helper T 17 cytokines or chemokines. The bar graph confirms that there are far more positive links and interactions, which supports the previous suggestion.

5.3 SUPPLEMENTARY DATA

5.3.1 PEARSON CORRELATION PLOTS

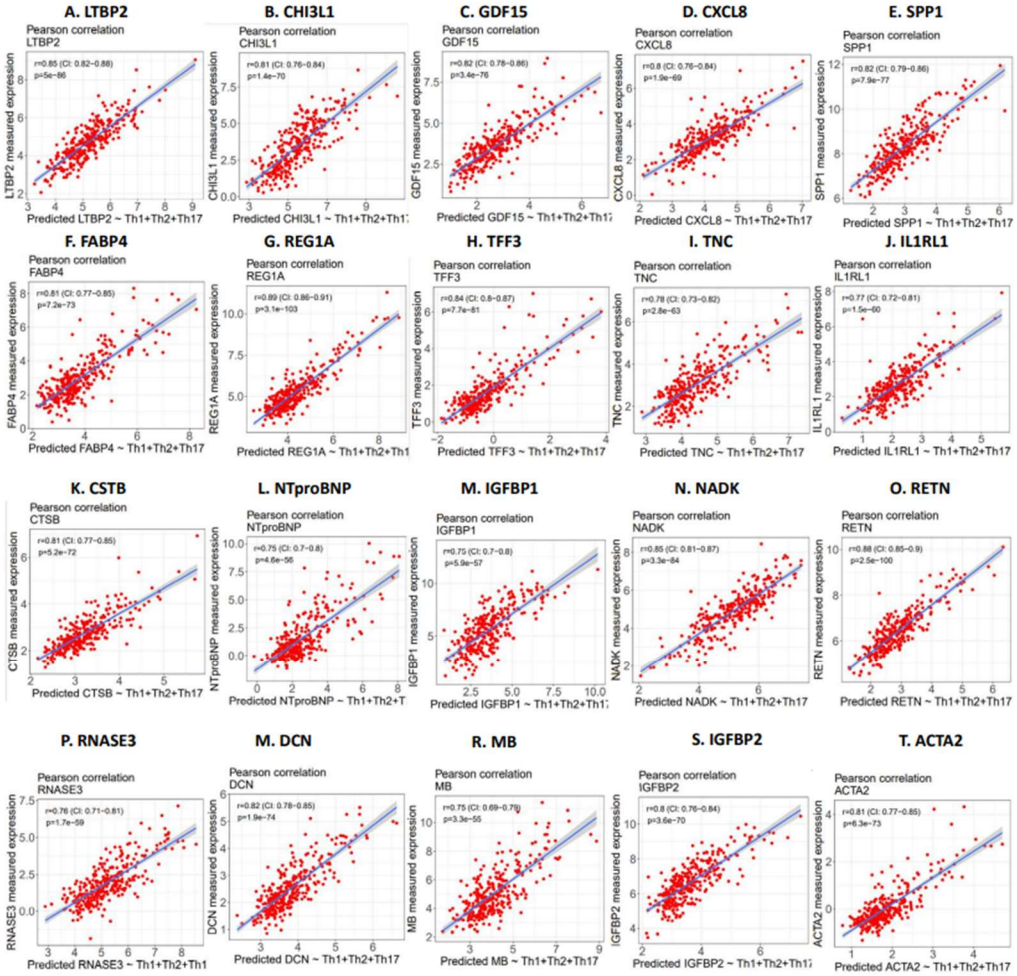

Figure 5.8: Pearson Scatter Plots

As part of supplementary data, scatter plots of the cardiometabolic protein Pearson correlations were generated, which show how strong the correlation is between the predicted cardiometabolic protein expression and the actual cardiometabolic protein expression. These scatter plots, shown in Figure 5.8, were generated for every cardiometabolic protein investigated in the study. In Figure 5.8, there are the scatter plots of twenty of the twenty-three significant

cardiometabolic proteins correlated with severity. All of these scatter plots feature positive correlation, showing that the expression is expected and this helps confirm that the data is precise. The Pearson correlation coefficient, r, measures how well a prediction model fits, with all r values in the figure being greater than 0.7. The corresponding p-value is included for each protein as well.

5.3.2 MEANS, logFCH, FCH, AND p-value TABLES

After the generation of visualized data forms such as heatmaps and networks, the rest of the data was put into tables, shown in Figure 5.9, 5.10, and 5.11, each concerning the Helper T associated cytokines or chemokines. The statistics displayed through these tables identify the mean expression of each cytokine or chemokine for each of the three patient groups and the logFCH, FCH, and p-values for all comparisons between the groups.

A. Th1

marker	Mean_Estimate_Deceased	Mean_Estimate_Intubated	Mean_Estimate_NonSevere	lgFCH_Deceased_vs_Intubated	FCH_Deceased_vs_Intubated	p_Deceased_vs_Intubated	lgFCH_Deceased_vs_NonSevere	FCH_Deceased_vs_NonSevere	p_Deceased_vs_NonSevere	lgFCH_Intubated_vs_NonSevere	FCH_Intubated_vs_NonSevere	p_Intubated_vs_NonSevere
CCL3	3.839667	3.758557	3.375698	0.08111	1.057832	0.632851	0.463969	1.379331	0.001702	0.382859	1.303923	0.001862
CCL4	4.533055	4.450697	4.183864	0.082358	1.058747	0.609644	0.349191	1.273846	0.012653	0.266833	1.203164	0.021959
CCL5	3.058536	3.497901	3.521671	-0.43937	-1.35601	0.089238	-0.46314	-1.37853	0.038352	-0.02377	-1.01661	0.898016
CXCL10	8.067081	8.027064	7.060412	0.040017	1.028126	0.869028	1.006669	2.009266	2.44E-06	0.966652	1.9543	6.45E-08
CXCL11	5.420621	5.473434	5.093661	-0.05281	-1.03729	0.79439	0.326961	1.254368	0.062564	0.379774	1.301138	0.009544
CXCL9	4.755986	4.626119	3.958236	0.129866	1.094192	0.541683	0.79775	1.738388	1.91E-05	0.667884	1.588741	1.71E-05
IFNG	2.912634	3.200185	3.559888	-0.28755	-1.22057	0.444137	-0.64725	-1.56618	0.047345	-0.3597	-1.28316	0.180299
IFNGR1	1.735405	1.364157	1.174299	0.371248	1.293471	0.000109	0.561105	1.475399	3.87E-11	0.189857	1.140651	0.005615
IFNGR2	2.288057	2.554254	2.214384	-0.2662	-1.20263	0.037079	0.073673	1.052393	0.502824	0.33987	1.265642	0.000239
IL1B	0.972867	0.715585	0.551015	0.257282	1.195224	0.027092	0.421851	1.339646	3.30E-05	0.16457	1.120832	0.049095
IL2RA	5.35906	5.168139	4.904144	0.190921	1.141492	0.145873	0.454916	1.370703	7.32E-05	0.263995	1.200799	0.005378

Figure 5.9: Helper T 1 Marker Supplemental Data

B. Th2

marker	Mean_Estimate_Deceased	Mean_Estimate_Intubated	Mean_Estimate_NonSevere	lgFCH_Deceased_vs_Intubated	FCH_Deceased_vs_Intubated	p_Deceased_vs_Intubated	lgFCH_Deceased_vs_NonSevere	FCH_Deceased_vs_NonSevere	p_Deceased_vs_NonSevere	lgFCH_Intubated_vs_NonSevere	FCH_Intubated_vs_NonSevere	p_Intubated_vs_NonSevere
CCL11	6.867267	6.340584	6.343758	0.526683	1.440613	0.000114	0.523509	1.437447	9.80E-06	-0.00317	-1.0022	0.973879
CCL13	6.441117	6.23976	6.163189	0.201357	1.149779	0.204937	0.277927	1.212452	0.043277	0.07657	1.054508	0.502207
CCL17	4.20771	4.247852	4.606879	-0.04014	-1.02822	0.845314	-0.39917	-1.31875	0.02533	-0.35903	-1.28256	0.015733
CCL22	5.19659	5.28663	5.448229	-0.09004	-1.0644	0.488051	-0.25164	-1.19056	0.025435	-0.1616	-1.11853	0.084137
CCL24	5.229133	4.652407	4.639222	0.576726	1.491461	0.031271	0.589911	1.505154	0.010901	0.013185	1.009181	0.9452
CCL26	1.947276	1.858636	1.743453	0.08864	1.063368	0.668685	0.203824	1.151747	0.255128	0.115183	1.083113	0.439454
CCL7	5.453148	5.706034	4.334088	-0.25289	-1.19159	0.35047	1.11906	2.172054	2.62E-06	1.371947	2.588195	1.18E-11
TSLP	0.124193	0.165269	0.166628	-0.04108	-1.02888	0.640193	-0.04244	-1.02985	0.576227	-0.00136	-1.00094	0.982833
IL10	0.392479	0.395799	0.121696	-0.00332	-1.0023	0.989468	0.270782	1.206462	0.213273	0.274102	1.209241	0.130328
IL13	-0.18518	-0.08663	-0.08922	-0.09855	-1.0707	0.303685	-0.09596	-1.06878	0.246463	0.00259	1.001797	0.969987
IL33	0.145867	0.17389	0.053408	-0.02802	-1.01961	0.716487	0.092459	1.066186	0.166098	0.120482	1.087098	0.030523
IL4R	3.974879	3.615075	3.073927	0.359804	1.283251	0.047431	0.900952	1.867297	1.97E-08	0.541148	1.45513	4.09E-05
IL5	0.087957	0.389097	0.188048	-0.30114	-1.23212	0.171847	-0.10009	-1.07184	0.598658	0.201049	1.149534	0.204498
IL7R	4.057112	3.708964	3.962354	0.348148	1.272925	0.008226	0.094758	1.067886	0.402652	-0.25339	-1.192	0.007484

Figure 5.10: Helper T 2 Marker Supplemental Data

C. Th17

marker	Mean_Estimate_Deceased	Mean_Estimate_Intubated	Mean_Estimate_NonSevere	lgFCH_Deceased_vs_Intubated	FCH_Deceased_vs_Intubated	p_Deceased_vs_Intubated	lgFCH_Deceased_vs_NonSevere	FCH_Deceased_vs_NonSevere	p_Deceased_vs_NonSevere	lgFCH_Intubated_vs_NonSevere	FCH_Intubated_vs_NonSevere	p_Intubated_vs_NonSevere
S100A12	6.28179	6.370781	5.712131	-0.08899	-1.06363	0.517601	0.569659	1.484173	2.50E-06	0.658649	1.578604	1.23E-10
S100P	2.406164	2.023994	1.42661	0.38217	1.303301	0.032771	0.979554	1.971856	7.32E-10	0.597384	1.51297	4.70E-06
CCL20	6.250036	5.6281	4.885216	0.621936	1.538939	0.0198	1.364819	2.575441	7.41E-09	0.742884	1.673518	0.000123
LCN2	3.086124	2.520122	2.200199	0.566001	1.480415	0.000796	0.885925	1.847949	2.61E-09	0.319923	1.248264	0.008147
PI3	2.858407	1.784919	1.671535	1.073488	2.104515	2.17E-05	1.186872	2.276586	7.24E-08	0.113384	1.081763	0.526691
CXCL1	3.875114	3.572672	3.533874	0.302443	1.233231	0.111447	0.34124	1.266845	0.037924	0.038798	1.027257	0.775992
CXCL3	4.791669	4.784497	5.078272	0.007172	1.004984	0.97909	-0.2866	-1.21976	0.225943	-0.29377	-1.22584	0.136135
IL12A	4.276736	4.333357	4.444208	-0.05662	-1.04003	0.782909	-0.16747	-1.12309	0.345851	-0.11085	-1.07987	0.453321
IL12B	5.547005	5.566451	5.679793	-0.01945	-1.01357	0.918413	-0.13279	-1.09641	0.4184	-0.11334	-1.08173	0.406623
IL17A	0.827764	0.410578	0.449506	0.417187	1.335321	3.26E-05	0.378258	1.299772	1.34E-05	-0.03893	-1.02735	0.584485
IL17F	0.561443	0.381466	0.410569	0.179977	1.132866	0.223551	0.150874	1.110242	0.237566	-0.0291	-1.02038	0.784056
IL6	7.188969	6.763184	5.177767	0.425785	1.343304	0.144768	2.011202	4.03118	2.80E-14	1.585417	3.000945	4.53E-13
IL6R	4.358988	4.280809	4.312342	0.078179	1.055685	0.402947	0.046646	1.032861	0.563405	-0.03153	-1.0221	0.638831

Figure 5.11: Th17 Supplemental Marker Data

From this data, the process behind the generation of the heatmaps can be seen, as this data is used during the generation of the heatmaps. The p-values are valuable as well, as they show that some comparisons may not be as significant. A statistically significant comparison is represented by a p-value less than 0.05. From this it can be seen that while some comparisons are not statistically significant, but a large number are.

CHAPTER 6

DISCUSSION AND FUTURE WORK

6.1 SIGNIFICANT CARDIOMETABOLIC PROTEINS IN DISEASE

Of the thirty-one cardiometabolic proteins that were noted for significant correlation with COVID-19 severities, twenty-three have been highlighted as examples of cardiometabolic proteins associated with involvement in cardiovascular-related diseases or, in the case of the cardiometabolic protein GPR37, cardiovascular development.

LTBP2 has been identified previously as a marker associated with human heart failure (Bai et al., 2012). CHI3L1 levels has been correlated with severity levels in coronary (Ściborski et al., 2020) and carotid atherosclerotic plaque (Michelsen et al., 2010) as well as stroke (Ridker et al., 2014). Elevated GDF15 levels have been associated with higher risks in multiple cardiovascular diseases such as stable coronary artery disease, acute coronary syndrome, and heart failure (Kempf et al., 2009). Elevated CXCL8 levels have been found, in previous research, in cases of atherosclerotic plaque (Rus et al, 1996). SPP1 expression has been found to be higher in response to ischemia associated with stroke (Zhu et al, 2017), myocardial infarction (Muller et al., 2011) and peripheral artery disease (Koshikawa et al., 2009). FABP4 has been found to contribute to the development of atherosclerosis, and studies shown that lower levels of FABP4 protect against atherosclerosis to a degree (Makowski et al., 2001).

REG1A has been shown to have high levels of expression in heart tissue of patients who died of myocardial infarction (Kiji et al., 2005). TFF3 levels in sera have been linked to the prediction of major adverse cardiovascular events in (Obendorf et al., 2015) as well as being identified as a possible biomarker for myocardial infarction (Fernández et al., 2020). Il19 has been found to have an athero-protective effect, with higher expression levels resulting in lower atherosclerotic plaque lesion area in mice (Ellison et al., 2014). TNC has been previously linked to many cardiovascular diseases in humans such as pulmonary thromboembolism (Celik et al., 2011) and hypertension (Schumann et al., 2010). IL1RL1 has been studied as a meaningful marker in cardiac disease, and found to have increased expression in the lungs in cases of heart failure (Domingo et al., 2018). IL1RL1, a protein associated with general inflammation and atherosclerosis, has also been shown to have significant upregulation in cases of both lesional and non-lesional Atopic Dermatitis compared to controls. (Pavel et al., 2019). CSTB has been identified as a relevant biomarker associated with chronic heart failure patients (Bouwens et al., 2019).

NTproBNP has been shown to be a reliable biomarker in diagnostic evaluation and outcome prediction in cases of acute heart failure, especially in dyspneic patients (Panagopoulou et al., 2013; Januzzi et al., 2006). One study suggested that NTproBNP been seen as “as S.O.S. signal” in heart failure, valvular heart diseases, pulmonary hypertension, and ACS. (Kimmenade et al., 2007). Higher IGFBP1 expression has been previously related to lessened cardiovascular risk factors and decreased presence of atherosclerosis in elderly patients (Janssen et al., 1998). RETN has been implicated as a risk factor for cardiovascular diseases in patients with type 2 diabetes (Menzaghi et al., 2013).

RNASE3 studies shown that depletion of RNASE3 lead to development of heart disfunctions and induced apoptosis (Yamaguchi et al., 2004). DCN has been shown to play a protective role against cardiac diseases such as atherosclerosis and myocardial infarction, where DCN was found to reduce atherosclerosis development when overexpressed (Al Haj Zen et al., 2006) and DCN was found to aid in proper fibrotic evolution in myocardial infarction (Weis et al., 2005). Research has not yielded significant findings concerning the relations of GPR37 to cardiovascular disease, but GPR37 does play a role in cardiovascular development, with a study on mice finding GPR37 and GPR37L1 contributing to sexual dimorphism of central cardiovascular control, controlling blood pressure in females and assisting cardiovascular response in males (Coleman et al., 2018).

IGFBP2 expression was investigated in a study on pulmonary artery hypertension, and it found that elevated IGFBP2 expression was associated with increased severity and mortality in pulmonary artery hypertension cases (Yang et al., 2020). ACTA2 has been implicated in cardiovascular disease, with a case study reporting how a mutation of ACTA2 led to pulmonary hypertension and persistent ductus arteriosus, implicating ACTA2 in a role of cardiovascular development (Meuwissen et al., 2013). Another study on ACTA2 mutations found that ACTA2 mutations can potentially lead to coronary artery disease, stroke, and Moyamoya disease (Guo et al., 2009). PLA2G2A elevated expression has been associated with calcific aortic valve stenosis in humans in previous research (Perrot et al., 2020).

Two other notable proteins, NAD Kinase (NADK) and Myoglobin (MB), are also notable for the significant functions they perform within the body, even if they are not correlated in some way with cardiovascular disease. NADK plays a role in cellular energy as it helps convert the cellular energy carrier nicotinamide adenine dinucleotide (NAD) into its phosphorylated version

NADP. MB plays a role in oxygen transport to the mitochondria of muscle cells through the use of an iron molecule near the center of the protein's structure. Both of these proteins are very essential to the body's functions and so the implications of NADK overexpression being correlated to intubation and MB overexpression being correlated to deceased cases can be an interesting point for future study.

In Figure 5.5, the networks of the twenty previously discussed proteins visualize what cytokines influence their expression. Notably, the most common Th1 cytokine influence by far is IFNGR1 present in seventeen of the twenty networks. The most common Th2 cytokine influences are CCL11 and CCL7, each being present in ten and eight, respectively, of the twenty networks. The most common Th17 cytokine influences include PI3 and LCN2, which both were present in ten of the twenty networks, in addition to IL6 which was present in eight of the twenty networks. The common cytokines or chemokines are significant as this information could illuminate what the key players are in the Helper T response with reference to cardiometabolic proteins.

6.2 FUTURE STUDY

After the recent publication of the researched described in this thesis (Michels et al, 2021), there are many paths that can be taken for future study. The same processing methods can be used on other datasets of COVID-19 Patients that have undergone the same OLINK proteomics assay. This would allow the results to be validated further or to see if there is a regional factor towards the body's cytokine and chemokine content, as the original study data acknowledges that the research was performed on a large, urban population. While the groups are large enough for the results to be considered statistically significant, larger groups of study would provide more data of interest.

Another further point of study is to use this process on the more recent variants of COVID-19, such as the Omicron and Delta variants, which have been rising in more recent outbreaks. These variants are characterized by higher transmissibility and lower lethality, which would postulate an interesting question as to if the results would differ from the original variant. The study of other variants would yield more information on how Helper T Cell cytokines and chemokines interact the cardiometabolic proteins and outcomes.

BIBLIOGRAPHY

Satiani B, Davis CA. PRACTICE MANAGEMENT the financial and employment effects of coronavirus disease 2019 on physicians in the United States 2020. doi:10.1016/j.jvs.2020.08.031.

Stenken J.A., Poschenrieder A.J. Bioanalytical chemistry of cytokines—A review. *Anal. Chim. Acta.* 2015;853:95–115. doi: 10.1016/j.aca.2014.10.009.

Del Valle, D. M. et al. An inflammatory cytokine signature predicts COVID-19 severity and survival. Nat. Med. (2020) doi:10.1038/s41591-020-1051-9.

Pavel, A et al. Th2/Th1 cytokine imbalance is associated with higher COVID-19 risk mortality. Frontiers in Genetics. Vol. 12. https://doi.org/10.3389/fgene.2021.706902

Dong, Ensheng, Hongru Du, and Lauren Gardner. "An interactive web-based dashboard to track COVID-19 in real time." The Lancet infectious diseases 20.5 (2020): 533-534.

Brobst B, Borger J. Benefits And Risks Of Administering Monoclonal Antibody Therapy For Coronavirus (COVID-19) [Updated 2022 Feb 6]. In: StatPearls [Internet]. Treasure Island (FL): StatPearls Publishing; 2022 Jan-. Available from: https://www.ncbi.nlm.nih.gov/books/NBK574507/?msclkid=d79f6779c4f611ec82fc5fd775efb3f7

Yang, Yang, et al. "Plasma IP-10 and MCP-3 levels are highly associated with disease severity and predict the progression of COVID-19." Journal of Allergy and Clinical Immunology 146.1 (2020): 119-127.

Guo T, et al. Cardiovascular implications of fatal outcomes of patients with coronavirus disease 2019 (COVID-19) *JAMA Cardiol.* 2020;5:811–818.

Yu, Wen-Liang, et al. "Cardiovascular complications of covid-19 and associated concerns: A review." Acta Cardiologica Sinica 37.1 (2021): 9.

Dong C. Cytokine Regulation and Function in T Cells. Annu Rev Immunol. 2021 Apr 26;39:51-76. doi: 10.1146/annurev-immunol-061020-053702. Epub 2021 Jan 11. PMID: 33428453.

Alberts B, Johnson A, Lewis J, et al. Molecular Biology of the Cell. 4th edition. New York: Garland Science; 2002. Helper T Cells and Lymphocyte Activation. Available from: https://www.ncbi.nlm.nih.gov/books/NBK26827/?msclkid=02d7190cc4f511eca92b11f48477963c

Wu Y, Huang X, Yuan L, Wang S, Zhang Y, Xiong H, Chen R, Ma J, Qi R, Nie M, Xu J, Zhang Z, Chen L, Wei M, Zhou M, Cai M, Shi Y, Zhang L, Yu H, Hong J, Wang Z, Hong Y, Yue M, Li Z, Chen D, Zheng Q, Li S, Chen Y, Cheng T, Zhang J, Zhang T, Zhu H, Zhao Q, Yuan Q, Guan Y, Xia N. A recombinant spike protein subunit vaccine confers protective immunity against SARS-CoV-2 infection and transmission in hamsters. Sci Transl Med. 2021 Aug 11;13(606):eabg1143. doi: 10.1126/scitranslmed.abg1143. Epub 2021 Jul 20. PMID: 34285130.

Khader SA, Gaffen SL, Kolls JK. Th17 cells at the crossroads of innate and adaptive immunity against infectious diseases at the mucosa. Mucosal Immunol. 2009 Sep;2(5):403-11. doi: 10.1038/mi.2009.100. Epub 2009 Jul 8. PMID: 19587639; PMCID: PMC2811522.

Ungar, Benjamin, et al. "COVID-19 symptoms are attenuated in moderate-to-severe atopic dermatitis patients treated with dupilumab." The Journal of Allergy and Clinical Immunology: In Practice 10.1 (2022): 134-142.

Fajgenbaum, David C, and Carl H June. "Cytokine Storm." *The New England journal of medicine* vol. 383,23 (2020): 2255-2273. doi:10.1056/NEJMra2026131

Kanehisa, M, and S Goto. "KEGG: kyoto encyclopedia of genes and genomes." *Nucleic acids research* vol. 28,1 (2000): 27-30. doi:10.1093/nar/28.1.27

Al-Kuraishy HM, Al-Gareeb AI, Al-Buhadily AK (2020). Cotrimoxazole and teicoplanin in the management of Covid-19: Pleiotropic effects, shadows and lights. Current Medical and Drug Research, 4 (2), Article ID 210

Olink Explore 1536 measures over 1500 proteins. Olink Explore 1536 measures over 1500 proteins. 2021.

Michael R. Filbin et al. Plasma proteomics reveals tissue-specific cell death and mediators of cell-cell interactions in severe COVID-19 patients. bioRxiv 2020.11.02.365536; doi: https://doi.org/10.1101/2020.11.02.365536

r-project.org. CRAN - Package glmnet (r-project.org). 2021

Igraph. igraph – Network analysis software. 2020.

Tidyverse. Create Elegant Data Visualisations Using the Grammar of Graphics • ggplot2 (tidyverse.org). No Date Stated.

Great Learning Team. *A complete understanding of lasso regression*. Great Learning Blog. Retrieved April 25, 2022, from https://www.mygreatlearning.com/blog/understanding-of-lasso-regression/?msclkid=bf863851c50011ecaf2a285d69a76bec

RDocumentation. *foldchange: Compute fold-change or convert between log-ratio and fold-change.* 2021. foldchange function - RDocumentation.

Tanha, Kiarash et al. "P-value: What is and what is not." *Medical journal of the Islamic Republic of Iran* vol. 31 65. 25 Sep. 2017, doi:10.14196/mjiri.31.65

Bai Y, Zhang P, Zhang X, Huang J, Hu S, Wei Y. LTBP-2 acts as a novel marker in human heart failure - a preliminary study. Biomarkers. 2012 Aug;17(5):407-15. doi: 10.3109/1354750X.2012.677860. Epub 2012 Apr 19. PMID: 22515403.

Ściborski K, Kuliczkowski W, Karolko B, Bednarczyk D, Protasiewicz M, Mysiak A, Negrusz-Kawecka M. Plasma YKL-40 levels correlate with the severity of coronary atherosclerosis assessed with the SYNTAX score. Pol Arch Intern Med. 2018 Nov 30;128(11):644-648. doi: 10.20452/pamw.4345. Epub 2018 Oct 10. PMID: 30303489.

Michelsen AE, Rathcke CN, Skjelland M, Holm S, Ranheim T, Krohg-Sørensen K, Klingvall MF, Brosstad F, Oie E, Vestergaard H, Aukrust P, Halvorsen B. Increased YKL-40 expression in patients with carotid atherosclerosis. Atherosclerosis. 2010 Aug;211(2):589-95. doi: 10.1016/j.atherosclerosis.2010.02.035. Epub 2010 Mar 4. PMID: 20347092.

Ridker PM, Chasman DI, Rose L, Loscalzo J, Elias JA. Plasma levels of the proinflammatory chitin-binding glycoprotein YKL-40, variation in the chitinase 3-like 1 gene (CHI3L1),

and incident cardiovascular events. J Am Heart Assoc. 2014;3(3):e000897. Published 2014 Jun 23. doi:10.1161/JAHA.114.000897

Kempf T, Wollert KC. Growth differentiation factor-15: a new biomarker in cardiovascular disease. Herz. 2009 Dec;34(8):594-9. doi: 10.1007/s00059-009-3317-3. PMID: 20024638.

Rus HG, Vlaicu R, Niculescu F. Interleukin-6 and interleukin-8 protein and gene expression in human arterial atherosclerotic wall. Atherosclerosis. 1996 Dec 20;127(2):263-71. doi: 10.1016/s0021-9150(96)05968-0. PMID: 9125317.

Zhu Q, Luo X, Zhang J, Liu Y, Luo H, Huang Q, Cheng Y, Xie Z. Osteopontin as a potential therapeutic target for ischemic stroke. Curr Drug Deliv. 2017; 14:766–772. doi: 10.2174/1567201814666161116162148

Muller O, Delrue L, Hamilos M, Vercauteren S, Ntalianis A, Trana C, Mangiacapra F, Dierickx K, De Bruyne B, Wijns W, Behfar A, Barbato E, Terzic A, Vanderheyden M, Bartunek J. Transcriptional fingerprint of human whole blood at the site of coronary occlusion in acute myocardial infarction. EuroIntervention. 2011; 7:458–466. doi: 10.4244/EIJV7I4A75

Koshikawa M, Aizawa K, Kasai H, Izawa A, Tomita T, Kumazaki S, Tsutsui H, Koyama J, Shimodaira S, Takahashi M, Ikeda U. Elevated osteopontin levels in patients with peripheral arterial disease. Angiology. 2009; 60:42–45. doi: 10.1177/0003319708314250

Makowski L, Boord JB, Maeda K, Babaev VR, Uysal KT, Morgan MA, Parker RA, Suttles J, Fazio S, Hotamisligil GS, Linton MF. Lack of macrophage fatty-acid-binding protein aP2

protects mice deficient in apolipoprotein E against atherosclerosis. Nat Med. 2001 Jun;7(6):699-705. doi: 10.1038/89076. PMID: 11385507; PMCID: PMC4027052.

Kiji T, Dohi Y, Takasawa S, Okamoto H, Nonomura A, Taniguchi S. Activation of regenerating gene Reg in rat and human hearts in response to acute stress. Am J Physiol Heart Circ Physiol. 2005 Jul;289(1):H277-84. doi: 10.1152/ajpheart.01206.2004. Epub 2005 Mar 18. PMID: 15778284.

Florian Obendorf, Carsten Thilo Herz, Clemens Höbaus, Gerfried Pesau, Renate Koppensteiner, Gerit Schernthaner. Abstract 16877: High Serum Levels of Trefoil Factor 3 are Associated With an Increased Risk for Cardiovascular Events. 2015. doi:10.1161/circ.132.suppl_3.16877 https://www.ahajournals.org/doi/abs/10.1161/circ.132.suppl_3.16877

Fernández Cisnal A, García-Blas S, Valero E, Miñana G, Núñez J, Sanchis Forés J. Trefoil factor-3 and galectin-4 as new candidates for prognostic biomarkers in ST-segment elevation myocardial infarction. Rev Esp Cardiol (Engl Ed). 2020 May;73(5):418-420. English, Spanish. doi: 10.1016/j.rec.2019.10.008. Epub 2019 Nov 21. PMID: 31761572.

Ellison S, Gabunia K, Kelemen SE, England RN, Scalia R, Richards JM, Orr AW, Traylor JG Jr, Rogers T, Cornwell W, Berglund LM, Goncalves I, Gomez MF, Autieri MV. Attenuation of experimental atherosclerosis by interleukin-19. Arterioscler Thromb Vasc Biol. 2013 Oct;33(10):2316-24. doi: 10.1161/ATVBAHA.113.301521. Epub 2013 Aug 15. Erratum in: Arterioscler Thromb Vasc Biol. 2014 Jan;34(1):e1. Orr, Wayne [corrected to Orr, A Wayne]. PMID: 23950143; PMCID: PMC3950941.

Celik A, Kocyigit I, Calapkorur B, Korkmaz H, Doganay E, Elcik D, et al. Tenascin-C may be a predictor of acute pulmonary thromboembolism, J Atheroscler Thromb, 2011, vol. 18 (pg. 478-493)

Schumann C, Lepper PM, Frank H, Schneiderbauer R, Wibmer T, Kropf C, Stoiber KM, Rüdiger S, Kruska L, Krahn T, Kramer F. Circulating biomarkers of tissue remodelling in pulmonary hypertension. Biomarkers. 2010 Sep;15(6):523-32. doi: 10.3109/1354750X.2010.492431. PMID: 20528622.

Domingo A. Pascual-Figal, Maria T. Pérez-Martínez, Maria C. Asensio-Lopez, Jesús Sanchez-Más, Maria E. García-García, Carlos M. Martinez, Miriam Lencina, Ruben Jara, James L. Januzzi, Antonio Lax. Pulmonary Production of Soluble ST2 in Heart Failure. 2018. doi:10.1161/CIRCHEARTFAILURE.118.005488. https://www.ahajournals.org/doi/abs/10.1161/CIRCHEARTFAILURE.118.005488

Pavel A, et al. The proteomic skin profile of moderate-to-severe atopic dermatitis patients shows an inflammatory signature. American Academy of Dermatology. DOI: https://doi.org/10.1016/j.jaad.2019.10.039

Bouwens E, Brankovic M, Mouthaan H, Baart S, Rizopoulos D, van Boven N, Caliskan K, Manintveld O, Germans T, van Ramshorst J, Umans V, Akkerhuis KM, Kardys I. Temporal Patterns of 14 Blood Biomarker candidates of Cardiac Remodeling in Relation to Prognosis of Patients With Chronic Heart Failure-The Bio- SH i FT Study. J Am Heart Assoc. 2019 Feb 19;8(4):e009555. doi: 10.1161/JAHA.118.009555. PMID: 30760105; PMCID: PMC6405680.

Panagopoulou V, Deftereos S, Kossyvakis C, Raisakis K, Giannopoulos G, Bouras G, Pyrgakis V, Cleman MW. NTproBNP: an important biomarker in cardiac diseases. Curr Top Med Chem. 2013;13(2):82-94. doi: 10.2174/1568026611313020002. PMID: 23470072.

Januzzi JL, van Kimmenade RV, Lainchbury J, et al: NT-proBNP testing for diagnosis and short-term prognosis in acute destabilized heart failure: an international pooled analysis of 1,256 patients; the International Collaborative of NT-proBNP Study. Eur Heart J. 2006 Feb;27(3):330-337

Kimmenade V, Januzzi. The Importance of Amino-terminal pro-Brain Natriuretic Peptide Testing in Clinical Cardiology. Biomark Insights. 2007;1:143-155. Published 2007 Feb 7.

Janssen JA, Stolk RP, Pols HA, Grobbee DE, Lamberts SW. Serum total IGF-I, free IGF-I, and IGFB-1 levels in an elderly population: relation to cardiovascular risk factors and disease. Arterioscler Thromb Vasc Biol. 1998 Feb;18(2):277-82. doi: 10.1161/01.atv.18.2.277. Erratum in: Arterioscler Thromb Vasc Biol 1998 Jul;18(7):1197. PMID: 9484994.

Menzaghi C, Bacci S, Salvemini L, Mendonca C, Palladino G, Fontana A, De Bonis C, Marucci A, Goheen E, Prudente S, Morini E, Rizza S, Kanagaki A, Fini G, Mangiacotti D, Federici M, De Cosmo S, Pellegrini F, Doria A, Trischitta V. Serum resistin, cardiovascular disease and all-cause mortality in patients with type 2 diabetes. PLoS One. 2013 Jun 3;8(6):e64729. doi: 10.1371/journal.pone.0064729. PMID: 23755138; PMCID: PMC3670852.

Yamaguchi O, Watanabe T, Nishida K, et al. Cardiac-specific disruption of the c- raf-1 gene induces cardiac dysfunction and apoptosis. J Clin Invest. 2004;114(7):937-943. doi:10.1172/JCI20317

Al Haj Zen A, Caligiuri G, Sainz J, Lemitre M, Demerens C, Lafont A. Decorin overexpression reduces atherosclerosis development in apolipoprotein E-deficient mice. Atherosclerosis. 2006 Jul;187(1):31-9. doi: 10.1016/j.atherosclerosis.2005.08.023. Epub 2005 Sep 23. PMID: 16183063.

Weis SM, Zimmerman SD, Shah M, Covell JW, Omens JH, Ross J Jr, Dalton N, Jones Y, Reed CC, Iozzo RV, McCulloch AD. A role for decorin in the remodeling of myocardial infarction. Matrix Biol. 2005 Jun;24(4):313-24. doi: 10.1016/j.matbio.2005.05.003. PMID: 15949932.

Coleman, J.L.J., Mouat, M.A., Wu, J. et al. Orphan receptor GPR37L1 contributes to the sexual dimorphism of central cardiovascular control. Biol Sex Differ 9, 14 (2018). https://doi.org/10.1186/s13293-018-0173-y

Yang, J., Griffiths, M., Nies, M.K. et al. Insulin-like growth factor binding protein-2: a new circulating indicator of pulmonary arterial hypertension severity and survival. BMC Med 18, 268 (2020). https://doi.org/10.1186/s12916-020-01734-3

Meuwissen ME, Lequin MH, Bindels-de Heus K, Bruggenwirth HT, Knapen MF, Dalinghaus M, de Coo R, van Bever Y, Winkelman BH, Mancini GM. ACTA2 mutation with childhood cardiovascular, autonomic and brain anomalies and severe outcome. Am J Med Genet A. 2013 Jun;161A(6):1376-80. doi: 10.1002/ajmg.a.35858. Epub 2013 Apr 23. PMID: 23613326.

Guo DC, Papke CL, Tran-Fadulu V, et al. Mutations in smooth muscle alpha-actin (ACTA2) cause coronary artery disease, stroke, and Moyamoya disease, along with thoracic aortic disease. Am J Hum Genet. 2009;84(5):617-627. doi:10.1016/j.ajhg.2009.04.007

Perrot N, Thériault S, Rigade S, et al. Lipoprotein-associated phospholipase A2 activity, genetics and calcific aortic valve stenosis in humans Heart 2020;106:1407-1412.

Michels JR, Nazrul MS, Adhikari S, Wilkins D, Pavel AB. Th1, Th2 and Th17 inflammatory pathways predict cardiometabolic protein expression in serum of COVID-19 patients. https://pubs.rsc.org/en/content/articlelanding/2022/MO/D2MO00055E